CHAPTER 2

Projected Drought for the Conterminous United States in the 21st Century

Matthew P. Peters
Louis R. Iverson

M.P. Peters is an Ecologist, U.S. Department of Agriculture, Forest Service, Northern Research Station, Northern Institute of Applied Climate Science, Delaware, OH 43015.

L.R. Iverson is a Landscape Ecologist, U.S. Department of Agriculture, Forest Service, Northern Research Station, Northern Institute of Applied Climate Science, Delaware, OH 43015.

BACKGROUND

Measuring and Defining Long-Term Trends of Drought

Several metrics are used to quantify the lack of available water in an environment and identify drought occurrences. Each metric focuses on different effects of water deficits, such as agricultural, meteorological, hydrological, ecological, or socioeconomic drought (Vose et al. 2016). Thirteen drought indices were developed and used in the United States in the 20th century, and some are still commonly used (Heim 2002). Zargar et al. (2011) described 74 indices used to characterize droughts.

Many of the climatic parameters needed to calculate these indices are based on observed values and are available in digital formats at fine spatial resolutions (Abatzoglou 2013, Daly et al. 2008). Other parameters are downscaled from future projections at temporal resolutions, either monthly (Thrasher et al. 2013) or daily (Maurer et al. 2014). Indices that use remotely sensed data to document past or near real-time droughts are not suited to model potential future drought conditions. This chapter focuses on the climate-based indices most conducive to projecting future conditions.

Regardless of the metric used to define drought, the ability to access past and projected future climate data provides information for multiple types of users: modelers seeking to improve climatic models, researchers and decision makers who need assessments on the current and potential future vulnerability of sectors affected by droughts, and the interested public wanting information on how climatic conditions may change. Although much research has focused on future changes in precipitation and temperature, few studies have examined potential changes in drought events for the United States (but see Cook et al. 2015, Dai 2012, Ryu and Hayhoe 2017). Regardless of scale, it is a challenging task to model complex, interconnected processes that regulate climatic patterns. Although modeling outputs may not align precisely with observed data, the resulting general trends provide insights into aspects of the climate system that influence observed changes and thus help to improve and refine modeling techniques (Hoskins et al. 2008). Individual and ensembles of models that indicate repeated periodic extreme events for one or more locations help to develop risk assessments (O'Neill et al. 2017).

In this chapter, we present some of the challenges associated with spatial modeling of drought in the past and into the future, and we examine some potential results from downscaled projections for the conterminous United States. The results are presented for the seven geographic regions used by the most recent U.S. National Climate Assessment (USGCRP 2017).

INDICES AND CLIMATIC DRIVERS FOR EXAMINING DROUGHT

Several indices related to drought are derived from climatic information; some also require soil properties. Examples include precipitation only (McKee et al. 1993), precipitation and temperature (Heddinghaus and Sabol 1991, Palmer 1965), precipitation and soil moisture (Keetch and Byram 1968, McGuire and Palmer 1957), and precipitation, temperature, and soil moisture (van der Schrier et al. 2013, Wells et al. 2004). These examples are not exhaustive, but they are generally the better known and more widely used indices applied in the United States and elsewhere.

Palmer Drought Severity Index

The Palmer Drought Severity Index (PDSI) (Palmer 1965) has been widely used to incorporate precipitation and temperature into a water balance model to classify meteorological and hydrological droughts. In response to criticisms of spatial incomparability on the original PDSI (Alley 1984, Guttman et al. 1992), it was modified by Heddinghaus and Sabol (1991) and updated by Wells et al. (2004) to account for local normal conditions via a self-calibrating approach.

Potential evapotranspiration (PET) is used to determine how much soil moisture could be lost under specified temperature conditions. Potential evapotranspiration is used by PDSI and other indices (e.g., standardized precipitation evapotranspiration index [Vicente-Serrano et al. 2010], moisture index [Koch et al. 2013]). Opinions vary on the best way to calculate PET. A key issue is whether temperature-only-based methods (e.g., Thornthwaite 1948) are sufficient, or if process-based methods like the Penman-Monteith model (Burke et al. 2006) are needed. Another issue is whether solar radiation and vapor pressure deficit are needed to calculate PET, especially when predicting future climate model outputs. Both Dai (2011) and van der Schrier et al. (2013) swapped the Thornthwaite model with the Penman-Monteith model and found little effect on the resulting classification of drought by the PDSI. However, Milly and Dunne (2017) conducted a comprehensive study of several methods of calculating PET and projecting into the future on a global scale. For the period 1981–2000 compared to a multi-model mean, temperature-based methods of calculating evapotranspiration resulted in future projections with a higher percentage of change, and process-based methods (e.g., Penman-Monteith) had a lower percentage of change. We chose to use the Penman-Monteith approach to calculating PET because it is less biased than other methods.

Limitations and challenges with PDSI and time-series data—Palmer's (1965) original equation used the Thornthwaite (1948) method to calculate PET, where temperatures below 32 °F do not result in positive values of PET. The PDSI in this case therefore assumes that evapotranspiration does not occur under freezing conditions. However, PDSI is usually calculated using weekly or monthly climate data, and temperatures can fluctuate (above and below freezing) on smaller time scales. Therefore, snowmelt functions have been incorporated to account for delayed changes in soil moisture (Dai et al. 2004, Yan et al. 2014). These functions generally accumulate a snowpack when monthly temperatures are <32 °F and release a portion of the stored water when monthly temperature is above some threshold, usually above freezing.

Another common issue with many of the currently used drought and aridity indices (e.g., PDSI, standardized precipitation evapotranspiration index) is that they produce location-based, time series datasets that are not conducive for examining and interpreting thousands of locations over multiple periods. We sought a method to simply evaluate long-term drought that could be applied across the conterminous United States at a relatively fine scale. As a historic example, Marcovitch (1930) measured the severity of drought as a function of the length of consecutive days with temperatures >90 °F, weighted by total monthly precipitation for the period June through September. This index results in a single value that was originally intended to define conditions that were favorable or unfavorable for the Mexican bean beetle (*Epilachna varivestis*), but it could also be modified to represent normal conditions by averaging among many years. Although interesting, this index has limited value because an arbitrary threshold of 90 °F is used to define drought, but this criterion ignores soil moisture or water-holding capacity. Nonetheless, the notion of combining multiple time slices (e.g., months) has merit when visually representing drought conditions, which we sought to replicate in the analysis reported here. By aggregating time series data into a weighted value, such as the frequency of drought events weighted by their intensity, a single value can represent the relative droughtiness of a location over a given time.

In this chapter, we present indices that capture past and projected future drought periods as well as potential periods of excessive moisture. We present these indices for each of four 30-year periods from 1980 to 2099, showing the projected increase in drought conditions over much of the conterminous United States, especially under climate change scenarios with higher levels of greenhouse gas emissions (e.g., RCP 8.5, in which humans do not aggressively pursue a substantial reduction of inputs that influence atmospheric warming).

Cumulative Drought and Moisture Severity Indices

Two cumulative indices, the cumulative drought severity index (CDSI) and the cumulative moisture severity index (CMSI), were derived from the frequency of monthly drought (CDSI) and excessive moisture (CMSI) events, weighted by their intensity (Peters et al. 2015). Intensity was defined by seven self-calibrated PDSI (scPDSI) classes (Wells et al. 2004), three of drought, three of excessive moisture, and one of normal moisture. To represent the increase of intensity, each cumulative month received a weighting. Extreme drought (scPDSI <-3.9) or extremely moist (scPDSI >3.9) received a weighting of 3; severe drought (scPDSI -3.9 to -3.0) or a very moist spell (scPDSI 3.0 to 3.9) received a weighting of 2; moderate drought (scPDSI -2.9 to -2.0) or unusually moist spell (scPDSI 2.0 to 2.9) received a weighting of 1. Normal conditions were assumed when monthly scPDSI values ranged from -1.9 to +1.9 and received a zero weighting. Using the four 30-year periods of 1980–2009, 2010–2039, 2040–2069, and 2070–2099, CDSI and CMSI values were calculated from monthly scPDSI data derived from the climate and drought indices tools (National Integrated Drought Information System 2018) and accumulated for the 360 months in each 30-year period. The calibration period (1960–2010) can also influence the later periods by truncating the range of conditions representative of "normal" for a location, resulting in more extreme conditions (Dai and Zhao 2017). For this chapter, we examined how conditions might differ going forward for trees that were established over the last few decades (1960–2010).

Data Sources

Climate: current and future projections—Monthly precipitation, temperature, and mean PET were acquired from the climate data prepared for the Resources Planning Act (RPA) 2020 Assessment (Joyce et al. 2018). These data included the general circulation model (GCM) and representative concentration pathway (RCP) combinations of HadGEM2-ES365 4.5 (Had 4.5) and 8.5 (Had 8.5), IPSL-CM5A-MR 8.5 (IPSL 8.5), and MRI-CGCM3 4.5 (MRI 4.5) for a historical period of 1960–2005. Projections were modeled for the period 2006–2099. These GCM-RCP combinations represent four potential future conditions: hot-wet (HW) (Had 4.5), hot-slightly dry (HSD) (Had 8.5), hot-dry (HD) (IPSL 8.5), and warm-wet (WW) (MRI 4.5). These projections were statistically downscaled by Abatzoglou and Brown (2012) to ~4-km^2 grids.

In addition to using the climate data to calculate monthly scPDSI values, mean 30-year total annual and summer (June/July/August) precipitation and summer maximum temperature values were summarized across the conterminous United States for the periods of 1980–2009, 2010–2039, 2040–2069, and 2070–2099.

Soil-available water supply—Soil-available water supply (AWS) to a depth of 59 inches was obtained from the State soil survey geographic database (STATSGO) and aggregated to approximately 2.5- x 2.5-mile grids (fig. 2.1). The self-calibrated PDSI algorithm (Wells et al. 2004) partitions the available soil moisture, a static variable, into two bins: a top layer having a capacity to hold 1 inch of soil moisture, and a lower layer equal to any remaining soil moisture. Incorporating information about the soil's capacity to hold water to a depth of 59 inches produces PDSI values that are more relevant to the impact of drought on tree species, which access soil moisture much deeper than most agricultural and grassland vegetation. Across the conterminous United States, AWS ranges from 0 to 32 inches, with generally higher values, >8 inches, in the Central Plains region and along portions of East and West coasts (fig. 2.1).

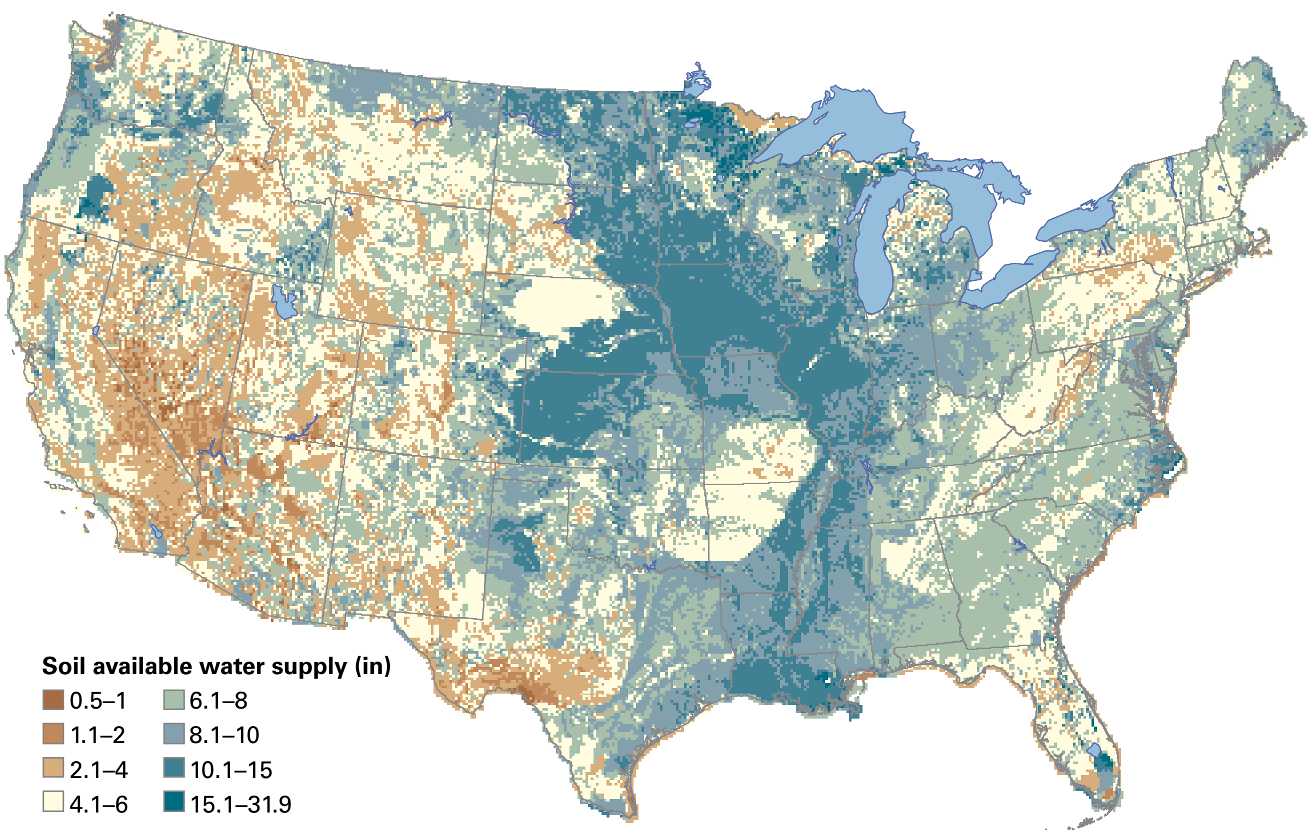

Figure 2.1—Soil-available water supply to a depth of 59 inches, derived from the U.S. Department of Agriculture, Natural Resources Conservation Service gridded State soil survey geographic database mapped across the conterminous United States at approximately 2.5- × 2.5-mile (1/24-degree) grids.

REGIONAL ANALYSES—ASSESSMENT OF TRENDS

To further evaluate the trends across the conterminous United States, we used the regions in the fourth National Climate Assessment (NCA4) (USGCRP 2017) to break out the patterns geographically with the drought inputs and indices. The NCA4 divides the United States into seven regions by State boundaries. For each, we present the mean values from four GCM-RCP scenarios for some precipitation, temperature, and drought metrics (tables 2.1–2.7).

Water Balance (Precipitation—Annual, June/July/August)

All seven U.S. regions show an increase in annual precipitation by the end of the 21st century for the WW, HW, and HSD scenarios, but a lessening of annual precipitation for all regions except the Northeast and Northwest under the HD scenario (tables 2.1–2.7). On the other hand, summer precipitation, most important for vegetative growth, is projected to decrease by the end of the century for almost all regions and scenarios except the WW scenario. As one example, in the Northern Plains under the HSD scenario, annual precipitation is projected to increase by 9.6 percent, but summer precipitation is projected to decrease by 28.7 percent; coupled with an 18.9-percent increase in temperature, this yields a 470-percent increase in the CDSI (table 2.3).

Although these increases in precipitation under the WW, HW, and HSD scenarios, if realized, could mitigate some of the effects of projected warmer temperatures, seasonal shifts in precipitation and reductions to snowpacks can exacerbate warming by reducing soil moisture at critical times in plant growth, producing physiological stress on plants. The rate at which precipitation is projected to change over the three periods varied among regions, where some regions are expected to experience increases in summer precipitation during the 2010–2039 period and then reductions during the middle and later portions of the century.

Summer Temperatures (Maximum Temperature—June/July/August)

All regions and all scenarios show marked increases in mean maximum summer temperatures, increasing throughout the century (tables 2.1–2.7). These increases were most severe in the HSD scenario (up to a 19.6-percent increase in the Northwest by 2099, rising from 77.7 to 92.9 °F), followed by HD, HW, and finally, WW, which had only a 2.6- to 4.3-percent increase in maximum summer temperatures. Each of the seven U.S. regions is projected to experience differences in the amount and rate of warming, especially under RCP 8.5, which may result in especially intensified drought conditions in some locations due to a concomitant reduction in summer precipitation. Northern regions are generally expected to experience larger changes in maximum summer temperatures by century's end (tables 2.1–2.4) compared to southern regions (tables 2.5–2.7). But because the southern zones are already relatively hot, conditions in these locations could become very stressful for many organisms, including humans, at times when monthly average maximum summer temperatures reach 100.6–105.4 °F (see also Matthews et al. 2018). Thus, the "hot droughts" already documented in the Southwest (Allen et al. 2015) will be exacerbated there and may be observed in other parts of the Nation.

Cumulative Drought Severity and Moisture Severity Indices (CDSI/CMSI)

Monthly scPDSI values, used to derive the CDSI and CMSI, were examined as a percentage of each region's area experiencing five conditions under the four GCM-RCP scenarios: extreme drought (scPDSI <-3.9), severe drought (-3.9 to -3.0), moderate drought (-2.9 to -2.0), near-normal (-1.9 to 1.9), unusual moist spell (2.0 to 2.9), very moist spell (3.0 to 3.9), and extremely moist (>3.9) (fig. 2.2). Figure 2.2 shows changes in PDSI among the four 30-year periods, with increased drought conditions during the two later periods (2040–2069, 2070–2099) for all regions. Concomitantly, except for three regions (Northern Plains, Southwest, Southeast) under the WW scenario, all regions and scenarios showed a decline in cumulative moisture severity by end of the 21st century (tables 2.1–2.7). Although drought frequency and/or intensity is projected to increase regardless of scenario over this century, reductions to the near-normal and moisture surplus conditions varied regionally and by scenario. The two wet scenarios (WW, HW) retain the most near-normal conditions, whereas the two dry scenarios (HSD, HD) vary among near-normal and moisture surplus conditions (fig. 2.2).

The CDSI was derived by weighting the frequency of monthly self-calibrated PDSI values representing drought conditions as moderate (1), severe (2), and extreme (3). Projections indicate more frequent and/

Table 2.1—Midwest region summary (range, mean, and percentage change from current) of annual and summer (June/July/August) precipitation, mean summer maximum temperature, cumulative drought severity index, and cumulative moisture severity index, for four 30-year periods (1980–2009, 2010–2039, 2040–2069, 2070–2099)

MIDWEST															
Potential future condition[a]	Annual precipitation (in)			Summer precipitation (in)			Summer temperature (°F)			Cumulative drought severity index			Cumulative moisture severity index		
	RANGE	MEAN	% CHANGE	RANGE	MEAN	% CHANGE	RANGE	MEAN	% CHANGE	RANGE	MEAN (median)	% CHANGE	RANGE	MEAN (median)	% CHANGE
1980–2009															
WW	20–52	35.4		8–15	11.6		69.0–91.5	82.4		4–247	75 (74)		2–227	76 (68)	
HW	21–53	35.3		8–15	11.5		69.3–92.6	83.1		9–185	99 (99)		38–291	146 (145)	
HSD	21–53	35.2		8–15	11.4		69.5–92.5	83.3		1–174	71 (67)		49–307	168 (169)	
HD	19–52	36.3		8–16	12.2		69.6–91.8	82.8		0–30	4 (3)		39–340	180 (185)	
2010–2039															
WW	21–52	36.5	3.0	7–15	12.0	3.0	69.7–91.8	82.9	0.7	-105–250	50 (46)	66.5	-138–180	34 (48)	45.0
HW	22–50	36.4	3.2	7–15	11.1	-3.8	71.9–96.5	86.2	3.8	-141–50	-40 (-35)	-40.1	-203–155	-36 (-40)	-24.8
HSD	20–55	37.1	5.2	7–14	10.9	-4.1	72.4–97.3	87.1	4.6	-147–110	-31 (-37)	-43.7	-128–129	-40 (-45)	-24.0
HD	19–49	34.8	-4.1	7–15	10.9	-10.8	71.1–94.8	85.4	3.1	-12–61	9 (4)	225.5	-177–84	-62 (-65)	65.8
2040–2069															
WW	21–53	38.0	7.3	9–17	13.0	11.8	71.6–93.2	84.1	2.1	-163–147	32 (40)	42.7	-147–231	37 (36)	49.0
HW	19–55	37.3	5.8	7–14	10.0	-13.4	74.2–100.2	89.9	8.2	-106–308	26 (11)	26.2	-270–50	-83 (-84)	-57.0
HSD	20–49	35.3	0.2	5–12	8.5	-25.3	75.7–105.7	92.8	11.5	-65–283	59 (51)	82.2	-288–61	-128 (-133)	-76.2
HD	19–50	34.1	-5.9	6–14	10.2	-16.1	75.3–98.7	89.6	8.2	3–181	54 (45)	1,388.4	-305–24	-144 (-149)	-80.3
2070–2099															
WW	21–51	36.4	2.6	8–16	12.1	4.2	73.2–93.9	85.3	3.5	-97–244	98 (100)	131.5	-169–186	-3 (-1)	-4.2
HW	19–54	37.1	5.1	6–15	10.2	-11.5	77.2–101.7	92.3	11.1	-67–283	80 (77)	81.3	-279–37	-83 (-81)	-57.20
HSD	21–54	38.4	9.0	5–12	8.4	-26.1	81.8–108.8	98.4	18.1	-29–342	125 (115)	175.2	-305–35	-121 (-123)	-72.10
HD	20–50	33.0	-9.2	6–12	9.4	-23.1	80.5–105.0	95.1	14.9	185–404	289 (281)	7,383.8	-340– -16	-167 (-171)	-92.90

[a] Potential future conditions (represented by corresponding climate scenarios):
WW=warm-wet (MRI-CGCM3 4.5), HW=hot-wet (HadGEM2-ES365 4.5), HSD=hot-slightly dry (HadGEM2-ES365 8.5), and HD=hot-dry (IPSL-CM5A-MR 8.5).

Table 2.2—Northeast region summary (range, mean, and percentage change from current) of annual and summer (June/July/August) precipitation, mean summer maximum temperature, cumulative drought severity index, and cumulative moisture severity index, for four 30-year periods (1980–2009, 2010–2039, 2040–2069, 2070–2099)

NORTHEAST															
Potential future condition[a]	Annual precipitation (in)			Summer precipitation (in)			Summer temperature (°F)			Cumulative drought severity index			Cumulative moisture severity index		
	RANGE	MEAN	% CHANGE	RANGE	MEAN	% CHANGE	RANGE	MEAN	% CHANGE	RANGE	MEAN (median)	% CHANGE	RANGE	MEAN (median)	% CHANGE
1980–2009															
WW	32–89	46		9–23	13		59.5–88.3	79.0		22–174	88 (89)		15–323	109 (104)	
HW	31–86	45		8–22	13		59.9–88.8	79.5		1–178	55 (55)		29–266	127 (123)	
HSD	31–86	45		8–23	12		60.0–89.0	79.7		0–192	33 (26)		16–241	96 (85)	
HD	32–89	46		8–23	12		59.9–88.6	79.4		0–58	10 (7)		60–284	136 (129)	
2010–2039															
WW	32–90	47	2.0	8–22	12	-5.4	60.6–89.6	79.7	0.9	-108–167	2 (-14)	2.3	-248–123	0 (6)	-0.3
HW	32–91	47	3.4	8–26	13	5.7	62.4–91.4	82.5	3.8	-104–119	7 (4)	12.3	-193–85	-26 (-15)	-20.7
HSD	33–93	49	8.4	8–24	13	3.5	62.6–91.8	82.7	3.7	-101–30	-8 (-5)	-23.4	-97–219	33 (34)	34.4
HD	32–86	45	-0.8	9–24	13	6.4	62.1–90.8	81.6	2.7	-30–121	23 (18)	224.8	-128–63	-27 (-29)	-19.6
2040–2069															
WW	31–88	46	-0.1	7–21	12	-7.0	61.9–91.0	81.1	2.6	-102–238	75 (74)	84.9	-298–114	-56 (-59)	-51.9
HW	32–95	48	6.0	7–26	12	-1.8	65.4–94.8	85.8	7.9	-125–159	65 (76)	117.0	-226–73	-74 (-78)	-58.6
HSD	30–93	46	3.6	6–25	12	-3.9	67.2–99.3	87.9	10.3	-27–213	95 (99)	291.0	-229–48	-63 (-48)	-64.9
HD	33–91	47	3.0	8–24	13	5.4	65.8–93.9	85.2	7.3	31–157	91 (92)	886.4	-220–26	-64 (-56)	-46.8
2070–2099															
WW	33–93	47	2.5	8–23	12	-3.2	62.5–91.4	81.7	3.4	-42–207	57 (47)	64.6	-219–100	-14 (-12)	-12.8
HW	33–92	47	5.3	8–26	13	1.2	67.6–96.7	87.9	10.7	-8–222	112 (111)	202.4	-215–66	-79 (-72)	-62.0
HSD	34–99	50	11.8	7–27	12	-1.5	74.3–104.4	94.5	18.6	12–280	176 (178)	538.9	-232–58	-49 (-32)	-50.8
HD	33–94	48	4.7	8–24	12	0.4	70.2–99.0	90.1	13.4	97–349	210 (210)	2,033.8	-247–53	-93 (-86)	-68.7

[a] Potential future conditions (represented by corresponding climate scenarios):
WW=warm-wet (MRI-CGCM3 4.5), HW=hot-wet (HadGEM2-ES365 4.5), HSD=hot-slightly dry (HadGEM2-ES365 8.5), and HD=hot-dry (IPSL-CM5A-MR 8.5).

Table 2.3—Northern Plains region summary (range, mean, and percentage change from current) of annual and summer (June/July/August) precipitation, mean summer maximum temperature, cumulative drought severity index, and cumulative moisture severity index, for four 30-year periods (1980–2009, 2010–2039, 2040–2069, 2070–2099)

NORTHERN PLAINS															
Potential future condition[a]	Annual precipitation (in)			Summer precipitation (in)			Summer temperature (°F)			Cumulative drought severity index			Cumulative moisture severity index		
	RANGE	MEAN	% CHANGE	RANGE	MEAN	% CHANGE	RANGE	MEAN	% CHANGE	RANGE	MEAN (median)	% CHANGE	RANGE	MEAN (median)	% CHANGE
1980–2009															
WW	5–106	18.8		2–14	6.6		53.2–90.9	80.8		20–230	118 (122)		5–176	61 (61)	
HW	5–106	19.3		2–15	6.6		54.3–91.4	81.0		1–165	54 (46)		18–197	83 (77)	
HSD	5–107	19.2		1–15	6.6		54.5–91.5	81.1		0–154	47 (33)		8–237	82 (75)	
HD	5–104	19.1		2–15	6.4		54.6–91.5	82.0		0–110	18 (12)		7–266	86 (79)	
2010–2039															
WW	5–106	19.2	2.2	2–14	6.8	1.9	54.9–91.7	81.9	1.4	-120–184	14 (10)	12.3	-98–97	-12 (-14)	-19.4
HW	6–104	20.7	7.4	2–14	6.8	2.4	57.7–94.4	84.4	4.2	-129–134	19 (24)	34.6	-141–177	22 (14)	26.9
HSD	6–110	21.3	10.6	2–14	7.0	5.7	57.1–95.0	84.6	4.2	-98–95	9 (8)	19.3	-174–163	36 (37)	43.6
HD	6–105	19.4	1.2	2–14	6.6	2.5	56.3–94.2	84.2	2.6	-34–84	16 (13)	88.4	-140–124	2 (3)	2.2
2040–2069															
WW	6–104	19.9	5.8	2–15	7.0	5.8	55.6–92.5	82.6	2.2	-119–196	30 (32)	25.7	-111–122	5 (4)	8.1
HW	5–112	20.3	5.2	2–13	5.9	-10.3	60.7–97.4	87.8	8.5	-83–243	107 (108)	198.3	-164–79	-26 (-16)	-31.5
HSD	6–111	20.3	5.5	1–11	5.4	-18.3	62.9–100.2	90.1	11.0	-31–194	90 (92)	190.3	-189–57	-46 (-40)	-56.1
HD	5–113	18.7	-2.5	2–13	5.5	-13.8	61.3–99.3	89.0	8.6	3–190	77 (72)	430.3	-239–64	-64 (-58)	-74.8
2070–2099															
WW	6–109	20.3	8.0	2–14	6.9	4.3	56.8–93.7	83.8	3.6	-137–204	39 (42)	32.8	-106–159	24 (24)	39.4
HW	5–113	20.2	4.9	1–12	5.5	-16.3	62.6–98.5	90.0	11.1	-37–351	155 (160)	288.2	-182–75	-47 (-44)	-57.0
HSD	5–112	21.1	9.6	1–10	4.7	-28.7	69.0–106.8	96.4	18.9	7–377	222 (243)	470.5	-237–91	-53 (-49)	-64.8
HD	5–113	18.6	-2.6	1–16	5.8	-10.1	65.7–104.6	93.3	13.8	33–476	271 (259)	1,510.8	-256–42	-71 (-64)	-82.8

[a] Potential future conditions (represented by corresponding climate scenarios):
WW=warm-wet (MRI-CGCM3 4.5), HW=hot-wet (HadGEM2-ES365 4.5), HSD=hot-slightly dry (HadGEM2-ES365 8.5), and HD=hot-dry (IPSL-CM5A-MR 8.5).

Table 2.4—Northwest region summary (range, mean, and percentage change from current) of annual and summer (June/July/August) precipitation, mean summer maximum temperature, cumulative drought severity index, and cumulative moisture severity index for four 30-year periods (1980–2009, 2010–2039, 2040–2069, 2070–2099)

NORTHWEST															
Potential future condition[a]	Annual precipitation (in)			Summer precipitation (in)			Summer temperature (°F)			Cumulative drought severity index			Cumulative moisture severity index		
	RANGE	MEAN	% CHANGE	RANGE	MEAN	% CHANGE	RANGE	MEAN	% CHANGE	RANGE	MEAN (median)	% CHANGE	RANGE	MEAN (median)	% CHANGE
1980–2009															
WW	6–249	34.8		1–17	3.5		39.9–91.8	77.3		4–155	65 (64)		12–242	104 (102)	
HW	6–239	33.1		1–18	3.3		40.0–92.7	77.7		11–169	78 (75)		18–209	89 (87)	
HSD	6–241	33.1		1–17	3.0		39.9–92.8	77.7		1–204	59 (60)		20–216	105 (107)	
HD	7–247	35.0		1–18	3.7		40.1–93.0	78.1		0–190	21 (17)		15–294	123 (120)	
2010–2039															
WW	6–247	34.6	-0.7	1–19	3.8	9.7	40.8–93.3	78.4	1.5	-110–108	11 (10)	17.2	-206–109	-35 (-35)	-34.3
HW	7–243	34.4	3.9	1–16	3.0	-7.1	43.5–96.2	81.2	4.5	-138–80	-30 (-31)	-38.7	-130–96	-28 (-35)	-31.7
HSD	7–247	35.9	8.5	1–15	3.0	-1.7	44.1–95.9	81.5	4.8	-170–113	-33 (-35)	-55.6	-197–148	-18 (-25)	-17.6
HD	7–247	35.1	0.4	1–18	4.0	9.0	42.6–94.8	80.3	2.8	-115–176	34 (26)	163.5	-175–74	-32 (-31)	-26.0
2040–2069															
WW	7–255	34.8	-0.1	1–18	3.6	3.0	42.0–94.6	79.6	3.0	-41–190	62 (62)	95.1	-189–89	-29 (-30)	-27.6
HW	6–253	34.9	5.5	1–13	2.7	-16.6	47.1–99.6	84.6	8.8	-98–140	38 (39)	48.9	-184–87	-32 (-31)	-36.4
HSD	7–257	34.8	5.2	1–14	2.4	-21.2	48.2–101.9	86.4	11.2	-144–196	41 (40)	70.5	-188–114	-68 (-67)	-65.2
HD	7–266	37.1	6.0	1–17	3.5	-4.2	46.6–99.8	84.6	8.3	-135–178	54 (52)	259.4	-253–185	-56 (-56)	-45.4
2070–2099															
WW	6–256	35.0	0.4	1–19	3.6	2.1	43.1–95.5	80.6	4.3	-35–230	89 (92)	136.2	-210–104	-24 (-24)	-22.7
HW	7–263	35.4	7.0	1–13	2.9	-10.9	48.3–101.6	86.4	11.2	-123–308	132 (130)	169.6	-165–169	-17 (-16)	-19.1
HSD	7–240	34.4	4.0	0–11	2.2	-28.8	54.6–108.2	92.9	19.6	-148–355	185 (180)	316.3	-210–218	-75 (-83)	-72.2
HD	8–257	36.8	5.0	1–20	3.9	7.5	50.3–103.9	88.5	13.3	-116–306	185 (190)	894.1	-269–126	-59 (-53)	-47.6

[a] Potential future conditions (represented by corresponding climate scenarios):
WW=warm-wet (MRI-CGCM3 4.5), HW=hot-wet (HadGEM2-ES365 4.5), HSD=hot-slightly dry (HadGEM2-ES365 8.5), and HD=hot-dry (IPSL-CM5A-MR 8.5).

Table 2.5—Southeast region summary (range, mean, and percentage change from current) of annual and summer (June/July/August) precipitation, mean summer maximum temperature, cumulative drought severity index, and cumulative moisture severity index for four 30-year periods (1980–2009, 2010–2039, 2040–2069, 2070–2099)

SOUTHEAST															
Potential future condition[a]	Annual precipitation (in)			Summer precipitation (in)			Summer temperature (°F)			Cumulative drought severity index			Cumulative moisture severity index		
	RANGE	MEAN	% CHANGE	RANGE	MEAN	% CHANGE	RANGE	MEAN	% CHANGE	RANGE	MEAN (median)	% CHANGE	RANGE	MEAN (median)	% CHANGE
1980–2009															
WW	36–95	52.4		8–29	14.5		69.7–93.7	89.5		16–256	103 (106)		0–253	83 (82)	
HW	37–93	51.1		9–29	13.7		70.6–94.9	90.5		4–270	91 (87)		18–272	120 (114)	
HSD	36–93	50.8		9–29	13.8		70.7–95.0	90.5		1–216	62 (54)		5–240	117 (113)	
HD	36–96	53.0		8–30	14.4		70.3–94.1	89.8		0–173	19 (7)		54–255	138 (130)	
2010–2039															
WW	36–94	53.0	1.2	8–32	14.6	0.6	70.4–94.5	90.1	0.6	-113–153	8 (8)	7.9	-169–146	-10 (-15)	-11.8
HW	37–93	50.7	-0.8	7–30	13.4	-1.8	73.9–98.5	93.7	3.6	-153–127	-6 (-8)	-6.2	-200–108	-54 (-51)	-44.9
HSD	40–105	55.5	9.1	8–30	14.2	3.1	74.2–98.7	93.8	3.7	-171–119	-10 (-6)	-17.0	-155–246	45 (47)	39.0
HD	36–91	49.8	-6.0	8–30	14.2	-1.4	72.6–97.0	92.2	2.6	-119–95	33 (39)	172.9	-188–41	-72 (-65)	-52.1
2040–2069															
WW	39–98	54.7	4.5	9–33	15.5	7.0	71.8–95.8	91.3	2.1	-149–147	19 (23)	18.8	-170–155	9 (15)	10.5
HW	38–104	53.5	4.7	6–30	12.4	-9.1	77.0–101.4	96.6	6.8	-105–240	53 (54)	58.4	-191–87	-37 (-33)	-30.7
HSD	36–96	48.7	-4.1	4–26	10.6	-22.9	81.0–106.6	100.6	11.2	-34–296	120 (122)	195.1	-225–58	-86 (-80)	-73.4
HD	36–92	48.5	-8.6	8–29	14.5	0.3	75.4–100.9	95.3	6.2	-72–221	110 (111)	572.5	-224–74	-72 (-61)	-52.6
2070–2099															
WW	37–101	55.8	6.6	8–35	15.1	3.9	72.1–96.3	91.8	2.6	-187–229	12 (-9)	11.9	-194–203	30 (36)	35.9
HW	37–104	53.9	5.4	6–27	12.5	-8.5	78.1–101.9	97.7	8.0	-63–278	51 (44)	56.7	-209–112	-49 (-41)	-40.9
HSD	37–99	51.1	0.4	5–23	10.5	-23.6	85.2–109.2	103.9	14.8	-63–352	154 (156)	250.1	-227–34	-93 (-86)	-79.7
HD	33–85	45.5	-14.1	7–30	13.2	-8.6	80.5–106.7	100.6	12.0	65–452	305 (319)	1,587.2	-253–19	-117 (-110)	-85.0

[a] Potential future conditions (represented by corresponding climate scenarios):
WW=warm-wet (MRI-CGCM3 4.5), HW=hot-wet (HadGEM2-ES365 4.5), HSD=hot-slightly dry (HadGEM2-ES365 8.5), and HD=hot-dry (IPSL-CM5A-MR 8.5).

Table 2.6—Southern Plains region summary (range, mean, and percentage change from current) of annual and summer (June/July/August) precipitation, mean summer maximum temperature, cumulative drought severity index, and cumulative moisture severity index for four 30-year periods (1980–2009, 2010–2039, 2040–2069, 2070–2099)

SOUTHERN PLAINS															
Potential future condition[a]	Annual precipitation (in)			Summer precipitation (in)			Summer temperature (°F)			Cumulative drought severity index			Cumulative moisture severity index		
	RANGE	MEAN	% CHANGE	RANGE	MEAN	% CHANGE	RANGE	MEAN	% CHANGE	RANGE	MEAN (median)	% CHANGE	RANGE	MEAN (median)	% CHANGE
1980–2009															
WW	8–68	29.6		4–17	8.7		74.5–102.8	93.0		23–260	127 (128)		12–166	81 (81)	
HW	8–67	29.1		3–17	8.1		75.4–103.3	93.8		60–254	137 (136)		3–182	86 (90)	
HSD	8–67	28.6		3–16	8.3		75.4–103.3	93.7		48–238	127 (126)		11–186	93 (94)	
HD	9–69	30.6		4–20	9.7		74.7–102.4	93.0		0–69	20 (17)		63–278	163 (162)	
2010–2039															
WW	8–69	30.0	1.2	4–20	9.5	9.3	75.4–103.7	93.7	0.8	-130–130	11 (12)	8.3	-144–131	-38 (-41)	-47.0
HW	8–66	30.1	3.5	3–16	7.8	-3.7	77.7–105.7	96.3	2.7	-150–43	-63 (-65)	-46.0	-125–130	-7 (-4)	-7.8
HSD	7–75	30.6	7.1	3–16	7.9	-5.3	78.8–106.7	97.1	3.6	-174–103	-39 (-32)	-30.7	-95–102	-5 (-6)	-5.4
HD	8–61	26.2	-14.6	3–16	8.0	-16.8	77.6–106.8	96.3	3.6	-2–143	50 (47)	253.4	-255–36	-119 (-122)	-73.0
2040–2069															
WW	8–72	31.8	7.6	4–22	10.3	18.8	77.8–105.4	95.2	2.4	-116–184	32 (31)	25.0	-80–133	9 (4)	11.3
HW	8–71	29.5	1.4	3–15	7.5	-7.8	79.3–107.1	98.6	5.2	-98–163	37 (43)	27.0	-150–71	-36 (-36)	-41.8
HSD	8–60	26.8	-6.2	3–14	5.8	-31.0	81.8–109.5	101.6	8.4	-21–280	131 (134)	102.8	-162–83	-63 (-73)	-67.6
HD	6–52	23.6	-23.1	3–15	7.4	-23.3	82.4–110.3	100.3	7.9	80–307	156 (152)	783.4	-254–-36	-140 (-139)	-85.5
2070–2099															
WW	10–68	31.3	5.7	4–19	9.5	10.2	76.9–105.5	95.7	2.9	-127–242	7 (3)	5.6	-128–134	-11 (-13)	-13.7
HW	9–72	31.2	7.3	4–17	8.1	-0.9	80.3–107.1	99.2	5.8	-139–144	1 (2)	1.0	-143–128	-16 (-20)	-18.9
HSD	8–67	29.9	4.6	4–15	6.8	-18.4	85.0–112.5	103.9	10.9	-108–253	57 (48)	44.6	-153–74	-43 (-37)	-46.0
HD	4–48	21.1	-31.0	2–13	6.4	-33.6	88.9–116.2	105.7	13.8	293–551	430 (433)	2,161.4	-277–-63	-158 (-155)	-97.0

[a] Potential future conditions (represented by corresponding climate scenarios):
WW=warm-wet (MRI-CGCM3 4.5), HW=hot-wet (HadGEM2-ES365 4.5), HSD=hot-slightly dry (HadGEM2-ES365 8.5), and HD=hot-dry (IPSL-CM5A-MR 8.5).

Table 2.7—Southwest region summary (range, mean, and percentage change from current) of annual and summer (June/July/August) precipitation, mean summer maximum temperature, cumulative drought severity index, and cumulative moisture severity index for four 30-year periods (1980–2009, 2010–2039, 2040–2069, 2070–2099)

SOUTHWEST															
Potential future condition[a]	Annual precipitation (in)			Summer precipitation (in)			Summer temperature (°F)			Cumulative drought severity index			Cumulative moisture severity index		
	RANGE	MEAN	% CHANGE	RANGE	MEAN	% CHANGE	RANGE	MEAN	% CHANGE	RANGE	MEAN (median)	% CHANGE	RANGE	MEAN (median)	% CHANGE
							1980–2009								
WW	3–166	16.5		0–17	3.5		51.7–114.2	86.8		24–308	143 (134)		2–189	65 (61)	
HW	2–159	16.0		0–15	3.0		52.0–114.8	87.6		4–342	126 (120)		6–193	63 (60)	
HSD	2–156	15.6		0–14	2.8		51.9–114.8	87.6		0–331	106 (96)		6–178	61 (59)	
HD	3–168	17.2		0–19	3.7		52.3–114.7	87.5		0–186	20 (6)		2–261	90 (88)	
							2010–2039								
WW	3–158	17.0	3.2	0–17	3.4	-2.8	52.8–115.8	88.0	1.4	-239–137	-15 (-9)	-10.4	-137–123	10 (11)	14.8
HW	3–165	17.1	6.9	0–15	3.1	5.1	55.5–117.5	90.4	3.2	-113–161	12 (13)	9.3	-86–158	25 (25)	38.6
HSD	3–175	17.6	13.0	0–14	3.0	7.9	55.7–117.6	90.8	3.6	-234–132	-21 (-20)	-20.1	-102–161	27 (25)	44.0
HD	3–163	17.9	4.0	0–19	4.1	10.2	54.3–116.5	89.4	2.1	-103–177	13 (5)	67.3	-113–142	19 (20)	21.0
							2040–2069								
WW	3–163	16.9	2.3	0–16	3.5	-1.7	53.9–116.9	89.4	2.9	-117–267	52 (48)	36.6	-153–109	-4 (-2)	-5.5
HW	3–159	16.8	4.7	0–19	3.1	5.1	58.3–119.7	92.8	6.0	-148–221	34 (40)	26.8	-153–79	-18 (-17)	-28.7
HSD	2–156	15.5	-0.3	0–14	2.8	-0.9	59.8–121.2	94.8	8.1	-75–277	100 (107)	95.1	-153–57	-34 (-32)	-55.4
HD	3–167	15.5	-9.7	0–12	2.8	-23.9	58.2–121.1	94.3	7.8	-42–298	124 (117)	629.1	-247–90	-56 (-54)	-62.6
							2070–2099								
WW	3–161	18.3	11.0	0–22	3.9	10.6	55.2–117.9	89.9	3.6	-209–184	-31 (-27)	-21.6	-152–155	8 (8)	12.8
HW	3–157	17.2	7.2	0–18	3.2	9.3	59.5–121.0	93.9	7.2	-165–307	58 (62)	45.6	-144–129	-9 (-8)	-13.8
HSD	3–163	17.4	11.8	0–15	3.1	9.5	63.4–124.7	98.4	12.3	-104–387	124 (119)	117.2	-155–193	-23 (-25)	-37.0
HD	3–168	15.0	-13.0	0–8	1.8	-50.0	61.5–124.5	98.5	12.6	-56–615	304 (284)	1,541.7	-261–92	-64 (-67)	-71.7

[a] Potential future conditions (represented by corresponding climate scenarios):
WW=warm-wet (MRI-CGCM3 4.5), HW=hot-wet (HadGEM2-ES365 4.5), HSD=hot-slightly dry (HadGEM2-ES365 8.5), and HD=hot-dry (IPSL-CM5A-MR 8.5).

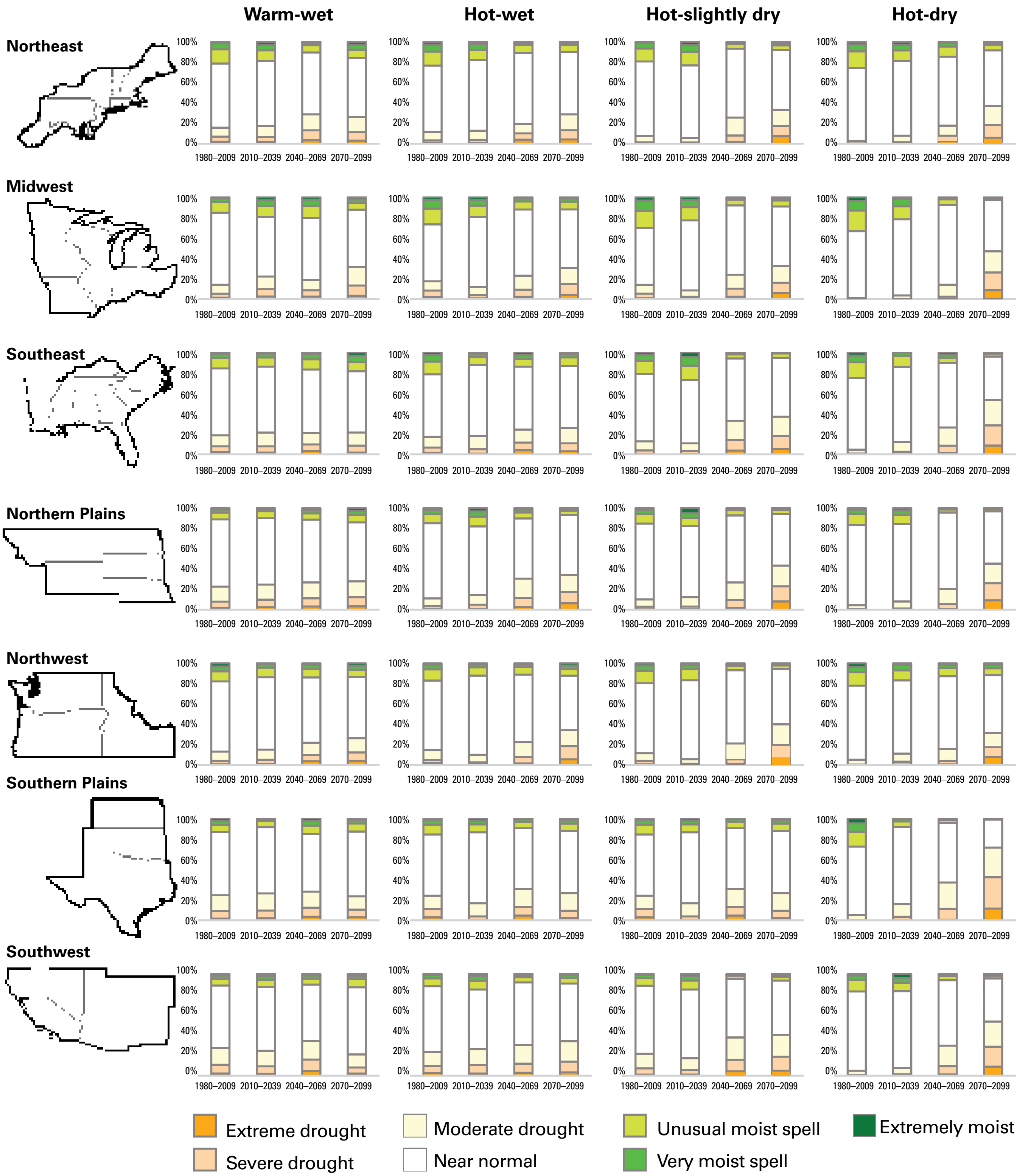

Figure 2.2—Palmer Drought Severity Index (PDSI) as the percentage of a 30-year period by area of each National Climate Assessment region, under four climate change scenarios (see text). Scenarios: warm-wet (WW), hot-wet (HW), hot-slightly dry (HSD), hot-dry (HD). Dates: historical (1980–2009), early century (2010–2039), mid-century (2040–2069), and late century (2070–2099).

or intense drought conditions in the conterminous United States by the end of the 21st century under all four GCM-RCP scenarios (tables 2.1–2.7). Compared to the baseline period, many regions could experience little change in droughts during 2010–2039, even under the two dry scenarios (HSD, HD) (figs. 2.5 and 2.6). However, CDSI values are projected to increase by middle to late century in all regions. Under the WW scenario, regional changes in CDSI in the first period (1980–2009) show either little change or some decreases (i.e., less drought), except in the Southern Plains and Southwest (fig. 2.3). Nevertheless, under all four GCM-RCP scenarios, the three later periods (2010–2039, 2040–2069, 2070–2099) project increases as much as <2 to thirteenfold by 2070 and <2 to seventy-threefold by 2100 with the HD scenario resulting in CDSI values much greater than twofold. The only exception is for the Southwest, which shows less drought in 2070–2099 under the WW scenario, despite sizeable increases in CDSI under the other three scenarios (tables 2.1–2.7). Under the two dry scenarios (HSD, HD), all regions show comparatively larger potential increases of CDSI for mid-century under the HSD scenario and for late century under the HD scenario, both indicating more drought if humans do not curtail greenhouse gas emissions.

The CMSI is the inverse of CDSI, weighting the frequency of monthly conditions with excess soil moisture. CMSI generally shows a lessening of excessive moisture conditions throughout the 21st century under the HW, HSD, and HD scenarios. However, the Midwest, Northeast, Northern Plains, and Southeast are projected to experience slight increases in the frequency and/or intensity of excess moisture conditions during the first period (1980–2009) (figs. 2.3–2.6), but stark reductions for the rest of the century (2010–2039, 2040–2069, and 2070–2099). Three regions could experience little change throughout the century: higher CMSI values for the WW scenario in the Northern Plains, Southeast, and Southwest. However, averaged across all regions, CMSI values are projected to decrease under all four scenarios by the end of the century.

DISCUSSION

Evaluating downscaled climate projections is a widely used practice to help inform management decisions and develop policies. However, uncertainties are associated with the GCMs, RCPs, and downscaling methods, and these must be considered when interpreting such data. Therefore, the model results and trends presented here are a guide, not precise trajectories. Nonetheless, the four GCM-RCP scenarios used in this evaluation represent bookends between warmer-to-hot and drier-to-wetter conditions. All scenarios show increasing maximum summer temperatures, sometimes by up to 15 °F.

Precipitation estimates are more uncertain in the climate models. For example, under the HSD scenario, the largest increases in annual precipitation are projected for the Northeast and Southwest regions during the last 30 years of the 21st century (2070–2099); this same scenario projects the lowest increases in annual precipitation in the Northwest and Southeast during the same period. All models suggest that important seasonal shifts in precipitation are likely, especially less precipitation during the summer months. Coupled with warmer summer temperatures, less summer precipitation could intensify and prolong physiological drought conditions, leading to additional tree mortality due to "hot droughts" (Allen et al. 2015).

Drought Projections

Based on projections from four GCM-RCP scenarios, the conterminous United States could experience much warmer temperatures and seasonal reductions in precipitation. The CDSI suggests that more frequent and/or intense droughts are likely in the middle to latter parts of the 21st century. Compared to the baseline period of 1980–2009, the 2010–2039 period shows little of the widespread increase in CDSI projected by the end of the century. Some regions may even experience fewer or less intense droughts during this period due to projected increases in precipitation. However, all regions show marked increases in drought conditions after 2040.

The models presented here use the process-based Penman-Monteith method to calculate PET. Although this method is less biased than others (Milly and Dunne 2017), it could show increasing uncertainty into the future because several of the underlying parameters (e.g., relative humidity, vapor pressure deficit) are modeled with uncertainty and at broad spatial scales. Therefore, these projections of CDSI also carry increasing uncertainty as we move into the latter decades of this century. Using four GCM-RCP scenarios, we have presented a range of possible drought conditions for the rest of the century. Regardless of scenario or region, however, drought conditions are likely to increase spatially and temporally.

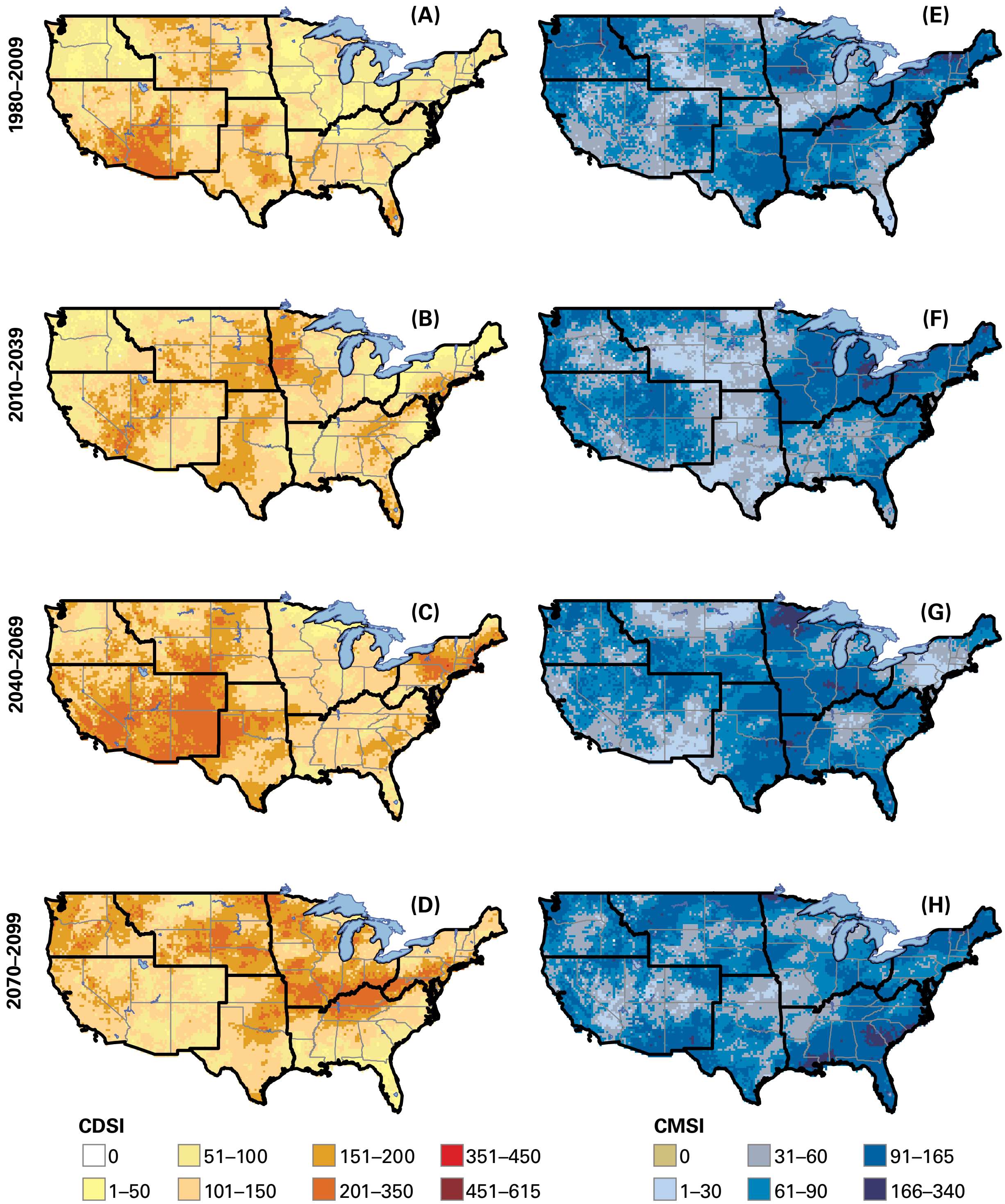

Figure 2.3—Cumulative drought severity index (CDSI) (A–D) and cumulative moisture severity index (CMSI) (E–H), derived from self-calibrated Palmer Drought Severity Index values calculated for the warm-wet (WW, MRI-CGCM3 4.5) scenario (see text). Changes in drought and moisture surplus, respectively, are shown for four 30-year periods: 1980–2009 (A,E), 2010–2039 (B,F), 2040–2069 (C,G), and 2070–2099 (D,H). National Climate Assessment regions are outlined in bold.

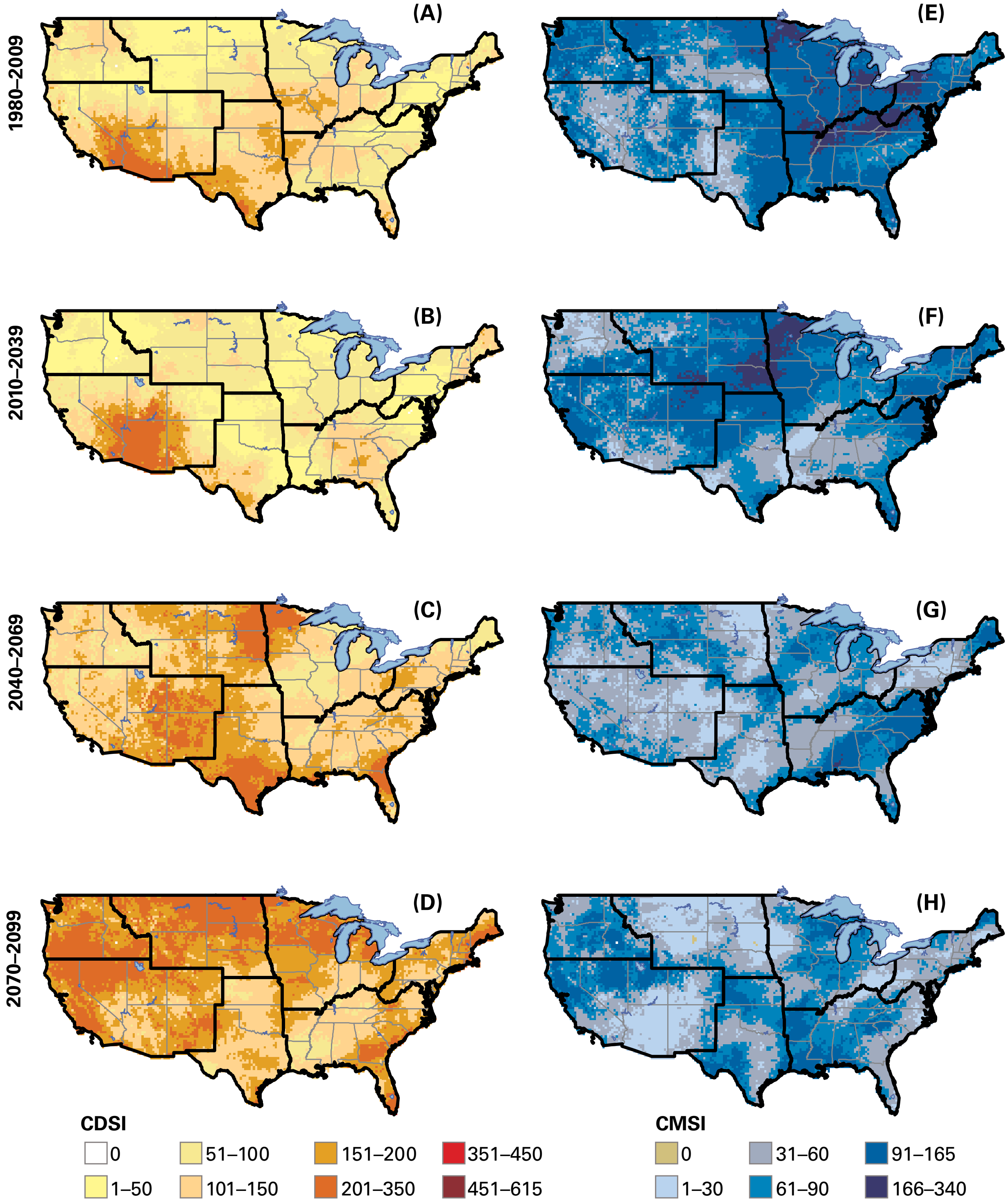

Figure 2.4—Cumulative drought severity index (CDSI) (A–D) and cumulative moisture severity index (CMSI) (E–H), derived from self-calibrated Palmer Drought Severity Index values calculated for the hot-wet (HW, HadGEM2-ES365 4.5) scenario (see tables). Changes in drought and moisture surplus, respectively, are shown for four 30-year periods: 1980–2009 (A,E), 2010–2039 (B,F), 2040–2069 (C,G), and 2070–2099 (D,H). National Climate Assessment regions are outlined in bold.

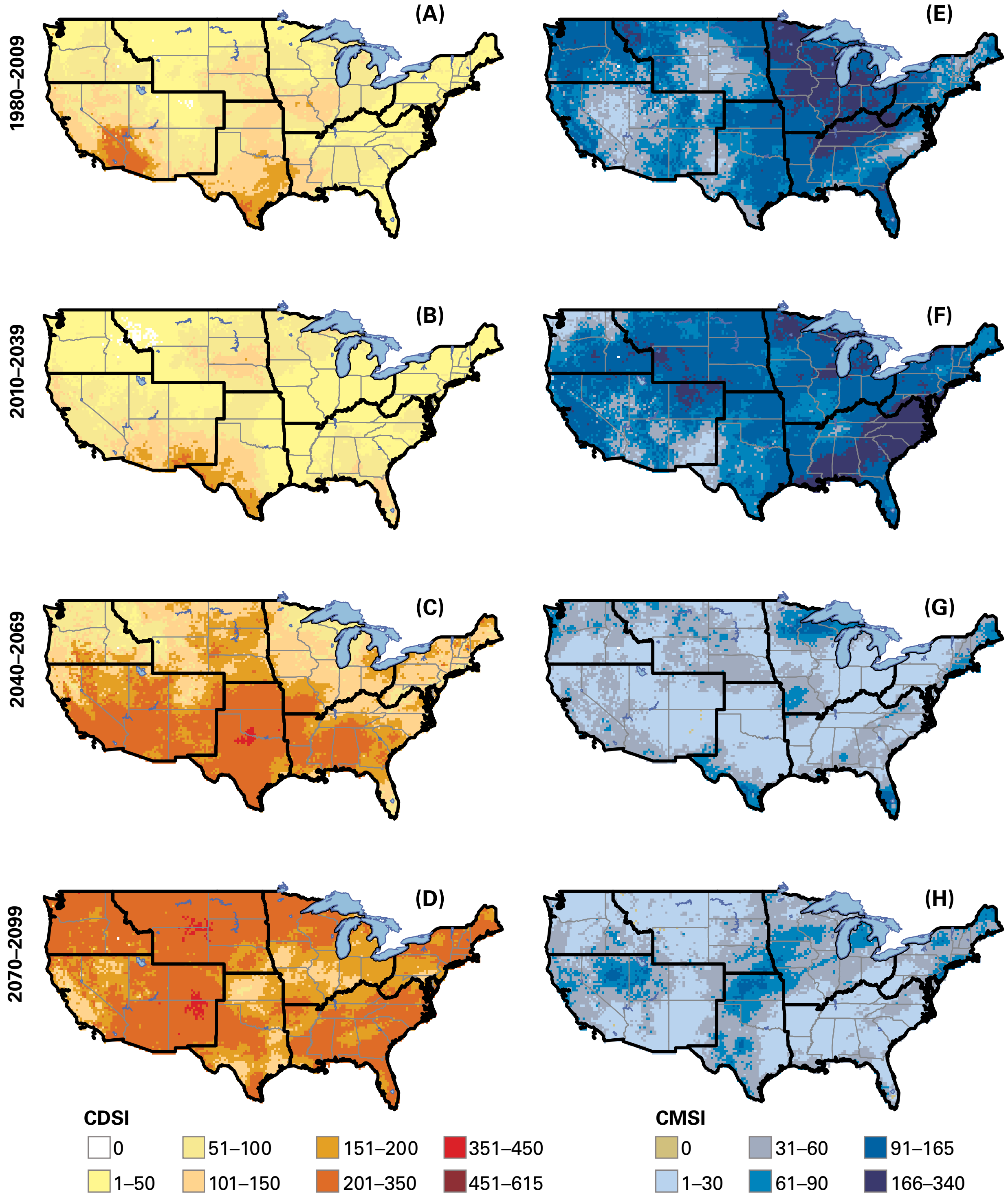

Figure 2.5—Cumulative drought severity index (CDSI) (A–D) and cumulative moisture severity index (CMSI) (E–H), derived from self-calibrated Palmer Drought Severity Index values calculated for the hot-slightly dry (HSD, HadGEM2-ES365 8.5) scenario (see tables). Changes in drought and moisture surplus, respectively, are shown for four 30-year periods: 1980–2009 (A,E), 2010–2039 (B,F), 2040–2069 (C,G), and 2070–2099 (D,H). National Climate Assessment regions are outlined in bold.

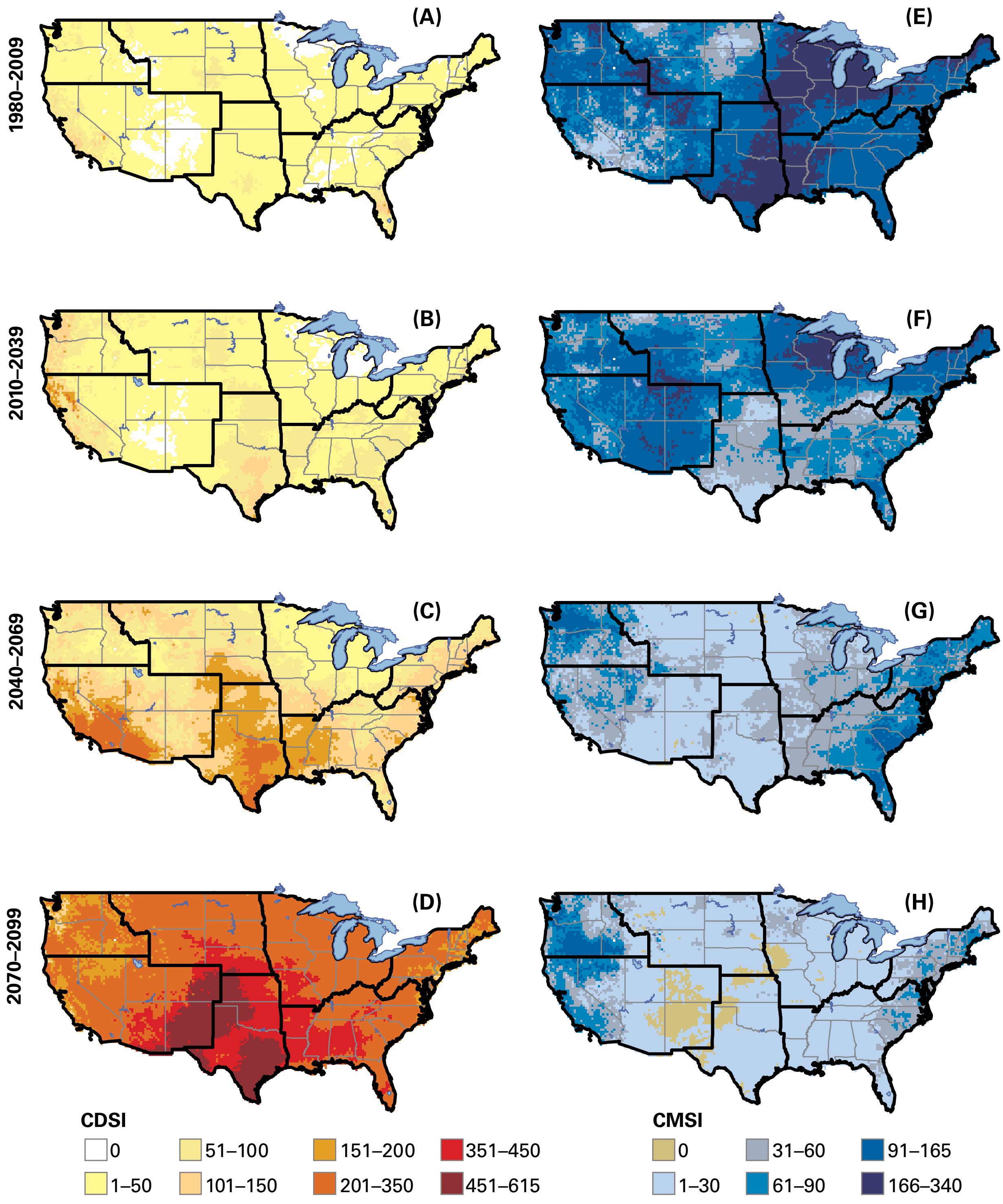

Figure 2.6—Cumulative drought severity index (CDSI) (A–D) and cumulative moisture severity index (CMSI) (E–H), derived from self-calibrated Palmer Drought Severity Index values calculated for the hot-dry (HD, IPSL-CM5A-MR 8.5) scenario (see text). Changes in drought and moisture surplus, respectively, are shown for four 30-year periods: 1980–2009 (A,E), 2010–2039 (B,F), 2040–2069 (C,G), and 2070–2099 (D,H). National Climate Assessment regions are outlined in bold.

Effects on Forests and Grasslands

Much of the literature on meteorological droughts focuses on soil moisture conditions within the top few inches, which is essential for shallow-rooted species, especially agricultural crops. However, the effects of drought differ for deep-rooted species such as trees and some grassland species. Therefore, it is important to consider a deeper soil moisture profile when parameterizing drought indices. We have attempted to address this issue by using a deeper soil horizon for soil-available water supply, but additional modifications may be necessary for this and other indices. The ability of trees to access water in deeper horizons during droughts is critical for survival.

Stress from drought can compound increased stress from other sources (e.g., competitors, disease, fire, pests), reducing the ability of trees to cope with overall physiological stress (Allen et al. 2015, Clark et al. 2016, Luce et al. 2016) and potentially resulting in the Manion decline spiral (Manion 1991). For example, the effects of drought and bark beetles on tree stress are well understood in the Western and Southeastern United States (Kolb et al. 2016). However, little is known about how forest composition in the Eastern United States might be affected by drought combined with insect outbreaks (e.g., Asian longhorned beetle [*Anoplophora glabripennis*], emerald ash borer [*Agrilus planipennis*], gypsy moth [*Lymantria dispar*], hemlock woolly adelgid [*Adelges tsugae*], mountain pine beetle [*Dendroctonus ponderosae*], southern pine beetle [*D. frontalis*]) and pathogens (e.g., oak wilt [*Ceratocystis fagacearum*], sudden oak death [*Phytophthora ramorum*], white pine blister rust [*Cronartium ribicola*]). Increasing numbers of nonnative species add to stress in native forests because nonnatives are often more competitive than natives during drought conditions. Although effects of drought on ecosystems in arid to semiarid regions of the Western United States have been well documented (Pederson et al. 2014), more droughts in the temperate Eastern United States in the future may produce novel climatic conditions and unknown effects on forests.

Concentrations of atmospheric CO_2 are expected to increase during the 21st century, although plant species responses over large regions to such increases is uncertain (Allen et al. 2015, Swann et al. 2016). This uncertainty can also influence the amount and even the direction of change for species evaluated in vulnerability assessments, depending on the metrics used to define drought conditions and the role of CO_2 enrichment in the analysis (Burke and Brown 2007, Swann et al. 2016).

Evaluation of GCM projections—Time will tell whether GCM projections are accurate, but regardless of the outcome, resource managers can make better informed decisions by examining a range of potential scenarios. The projections presented here include ranges of warming and wetting that are within the bounds of other model ensembles. Diversity of species composition and structure can help to reduce the overall effects of drought on forests (Clark et al. 2016). Therefore, evaluations of GCM projections should not only focus on how disturbances may change, but also consider which species might be favored by newly suitable habitat or increased resources (Iverson et al. 2008, 2011, 2017; Matthews et al. 2011).

Long-term soil moisture data—Some drought indices require information related to soil moisture, and spatial datasets related to soil characteristics are improving and becoming more available. Because of completeness and computational issues, we chose to use the older, coarse-level STATSGO data for the conterminous United States evaluation, and we found that it does not heavily influence the regional calculations of PDSI and CDSI/CMSI. This dataset does not provide long-term measures of soil moisture. Satellite-based imagery of soil moisture conditions can help to identify trends from around 1980 to the present (Nicolai-Shaw et al. 2017), but these data are of limited value in highly vegetated regions and represent only a series of snapshots along a timeline.

CONCLUSIONS

Analyzing future projections of drought under multiple climate change scenarios can provide insights on how regional temperatures, precipitation, and drought may change throughout this century, compared to baseline conditions of the period 1980–2009. The projections often show minimal changes in the next few decades, followed by large changes in the second half of the century. These changes will likely negatively affect plant growth and survival, leading to changes in forest composition and structure. These expected changes are larger under the two dry scenarios, especially the hot-dry scenario, emphasizing the value of reducing greenhouse gas emissions.

These projections of drought, considered in light of the model's uncertainties, can help managers prioritize strategies that may allow ecosystems to adapt to newer conditions. Forest management activities have the ability to shape the next forest over the course of this century, and the effects of different climate conditions must be considered to ensure that management goals are achieved.

LITERATURE CITED

Abatzoglou, J.T. 2013. Development of gridded surface meteorological data for ecological applications and modelling. International Journal of Climatology. 33: 121–131.

Abatzoglou, J.T.; Brown, T.J. 2012. A comparison of statistical downscaling methods suited for wildfire applications. International Journal of Climatology. 32: 772–780.

Allen, C.D.; Breshears, D.D.; McDowell, N.G. 2015. On underestimation of global vulnerability to tree mortality and forest die-off from hotter drought in the Anthropocene. Ecosphere. 6: 1–55.

Alley, W.M. 1984. The Palmer Drought Severity Index: limitations and assumptions. Journal of Climate and Applied Meteorology. 23: 1100–1109.

Burke, E.J.; Brown, S.J. 2007. Evaluating uncertainties in the projection of future drought. Journal of Hydrometerology. 9: 292–299.

Burke, E.J., Brown, S.J.; Christidis, N. 2006. Modeling the recent evolution of global drought and projections for the 21st century with the Hadley Centre climate model. Journal of Hydrometeorology. 7: 1113–1125.

Clark, J.S.; Iverson, L.; Woodall, C.W. 2016. Impacts of increasing drought on forest dynamics, structure, diversity, and management. In: Vose, J.M.; Luce, C.H.; Patel-Weynand, T., eds. Gen. Tech. Rep. WO-93b. Effects of drought on forests and rangelands in the United States: a comprehensive science synthesis. Washington, DC: U.S. Department of Agriculture, Forest Service, Washington Office: 59–96.

Cook, B.I.; Ault, T.R.; Smerdon, J.E. 2015. Unprecedented 21st century drought risk in the American Southwest and Central Plains. Science Advances. 1: e1400082.

Dai, A. 2011. Characteristics and trends in various forms of the Palmer Drought Severity Index during 1900–2008. Journal of Geophysical Research-Atmospheres. 116(D12).

Dai, A. 2012. Increasing drought under global warming in observations and models. Nature Climate Change. 3: 52–58.

Dai, A.; Trenberth, K.E.; Qian, T. 2004. A global dataset of Palmer Drought Severity Index for 1870–2002: relationship with soil moisture and effects of surface warming. Journal of Hydrometeorology. 5: 1117–1130.

Dai, A.; Zhao, T. 2017. Uncertainties in historical changes and future projections of drought. Part I: estimates of historical drought changes. Climatic Change. 144: 519–533.

Daly, C.; Halbleib, M.; Smith, J.I. [et al.]. 2008. Physiographically sensitive mapping of climatological temperature and precipitation across the conterminous United States. International Journal of Climatology. 28: 2031–2064.

Guttman, N.B.; Wallis, J.R.; Hosking, J.R.M. 1992. Spatial comparability of the Palmer Drought Severity Index. Journal of the American Water Resources Association. 28: 1111–1119.

Heddinghaus, T.R.; Sabol, P. 1991. A review of the Palmer Drought Severity Index and where do we go from here? In: Proceedings of the seventh conference on applied climatology. Boston: American Meteorological Society: 242–246.

Heim, R.R. 2002. A review of twentieth-century drought indices used in the United States. Bulletin of the American Meteorological Society. 83: 1149–1165.

Hoskins, B.; Schopf, P.; Navarra, A. 2008. Modelling the atmospheric, oceanic, and coupled system. In: Troccoli, A.; Harrison, M.; Anderson, D.L.T.; Mason, S.J., eds. Seasonal climate: forecasting and managing risk. Dordrecht, The Netherlands: Springer Science & Business Media: 127–161.

Iverson, L.; Prasad, A.M.; Matthews, S.; Peters, M. 2008. Estimating potential habitat for 134 eastern U.S. tree species under six climate scenarios. Forest Ecology and Management. 254: 390–406.

Iverson, L.; Prasad, A.M.; Matthews, S.; Peters, M. 2011. Lessons learned while integrating habitat, dispersal, disturbance, and life-history traits into species habitat models under climate change. Ecosystems. 14: 1005–1020.

Iverson, L.R.; Thompson, F.R.; Matthews, S. [et al.]. 2017. Multi-model comparison on the effects of climate change on tree species in the Eastern U.S.: results from an enhanced niche model and process-based ecosystem and landscape models. Landscape Ecology. 32: 1327–1346.

Joyce, L.A.; Abatzoglou, J.T.; Coulson, D.P. 2018. Climate data for RPA 2020 assessment: MACAv2 (METDATA) historical modeled (1950–2005) and future (2006–2099) projections for the conterminous United States at the 1/24 degree grid scale. Fort Collins, CO: U.S. Department of Agriculture, Forest Service research data archive. https://doi.org/10.2737/RDS-2018-0014. [Date accessed: June 21, 2018].

Keetch, J.J.; Byram, G.M. 1968. A drought index for forest fire control. Res. Pap. SE-38. Asheville, NC: U.S. Department of Agriculture, Forest Service, Southeastern Forest Experiment Station. 35 p.

Kolb, T.E.; Fettig, C.J.; Ayres, M.P. [et al.]. 2016. Observed and anticipated impacts of drought on forest insects and diseases in the United States. Forest Ecology and Management. 380: 321–334.

Luce, C.H.; Vose, J.M.; Pederson, N. [et al.]. 2016. Contributing factors for drought in United States forest ecosystems under projected future climates and their uncertainty. Forest Ecology and Management. 380: 299–308.

Manion, P. 1991. Tree disease concepts, 2d ed. Englewood Cliffs, NJ: Prentice Hall. 416 p.

Marcovitch, S. 1930. The measure of droughtiness. Monthly Weather Review. 58: 113.

Matthews, S.N.; Iverson, L.R.; Peters, M.P.; Prasad, A. 2018. Assessing potential climate change pressures across the conterminous United States: mapping plant hardiness zones, heat zones, growing degree days, and cumulative drought severity throughout this century. RMAP-NRS-9. Newtown Square, PA: U.S. Department of Agriculture, Forest Service, Northern Research Station. 31 p.

Matthews, S.N.; Iverson, L.R.; Prasad, A. [et al.]. 2011. Modifying climate change habitat models using tree species-specific assessments of model uncertainty and life history factors. Forest Ecology and Management. 262: 1460–1472.

Maurer, E.P.; Brekke, L.; Pruitt, T. [et al.]. 2014. An enhanced archive facilitating climate impacts and adaptation analysis. Bulletin of the American Meteorological Society. 95: 1011–1019.

McGuire, J.K.; Palmer, W.C. 1957. The 1957 drought in the Eastern United States. Monthly Weather Review. 85: 305–314.

McKee, T.B.; Doesken, N.J.; Kleist, J. 1993. The relationship of drought frequency and duration to time scales. In: Proceedings of the 8th conference on applied climatology. Boston: American Meteorological Society: 179–183.

Milly, P.C.D.; Dunne, K.A. 2017. A hydrologic drying bias in water-resource impact analyses of anthropogenic climate change. Journal of the American Water Resources Association. 53: 822–838.

National Integrated Drought Information System. 2018. Drought.gov. U.S. Drought Portal. Climate and drought indices in Python. https://www.drought.gov/drought/python-climate-indices. [Date accessed: June 22, 2018].

Nicolai-Shaw, N.; Zscheischler, J.; Hirschi, M. [et al.]. 2017. A drought event composite analysis using satellite remote-sensing based soil moisture. Remote Sensing of Environment. 203: 216–225.

O'Neill, B.C.; Oppenheimer, M.; Warren, R. [et al.]. 2017. IPCC reasons for concern regarding climate change risks. Nature Climate Change. 7: 28–37.

Palmer, W.C. 1965. Meteorological drought. Res. Pap. 45. Washington, DC: U.S. Department of Commerce, Weather Bureau. 58 p.

Pederson, N.; Dyer, J.M.; McEwan, R.W. [et al.]. 2014. The legacy of episodic climatic events in shaping temperate, broadleaf forests. Ecological Monographs. 84: 599–620.

Peters, M.P.; Iverson, L.R.; Matthews, S.N. 2015. Long-term droughtiness and drought tolerance of eastern U.S. forests over five decades. Forest Ecology and Management. 345: 56–64.

Ryu, J.-H.; Hayhoe, K. 2017. Observed and CMIP5 modeled influence of large-scale circulation on summer precipitation and drought in the South-Central United States. Climate Dynamics. 49: 4293–4310**.**

Swann, A.L.S.; Hoffman, F.M.; Koven, C.D.; Randerson, J.T. 2016. Plant responses to increasing CO^2 reduce estimates of climate impacts on drought severity. Proceedings of the National Academy of Sciences. 113: 10,019–10,024.

Thrasher, B.; Xiong, J.; Wang, W. [et al.]. 2013. Downscaled climate projections suitable for resource Management. Eos, Transactions American Geophysical Union. 94: 321–323.

Thornthwaite, C.W. 1948. An approach toward a rational classification of climate. Geographical Review. 38: 55–94.

USGCRP. 2017. Climate science special report: fourth National Climate Assessment, volume I. Wuebbles, D.J.; Fahey, D.W.; Hibbard, K.A. [et al.], eds. Washington, DC: U.S. Global Change Research Program. 470 p. doi: 10.7930/J0J964J6.

van der Schrier, G.; Barichivich, J.; Briffa, K.R.; Jones, P.D. 2013. A scPDSI-based global data set of dry and wet spells for 1901–2009. Journal of Geophysical Research: Atmospheres. 118: 4025–4048.

Vicente-Serrano, S.M.; Begueria, S.; Lopez-Moreno, J.I. 2010. A multiscalar drought index sensitive to global warming: the Standardized Precipitation Evapotranspiration Index. Journal of Climate. 23: 1696–1718.

Vose, J.M.; Clark, J.S.; Luce, C.H.; Patel-Weynand, T., eds. 2016. Effects of drought on forests and rangelands in the United States: a comprehensive science synthesis. Gen. Tech. Rep. WO-93b. Washington, DC: U.S. Department of Agriculture, Forest Service, Washington Office. 289 p.

Wells, N.; Goddard, S.; Hayes, M.J. 2004. A self-calibrating Palmer Drought Severity Index. Journal of Climate. 17: 2335–2351.

Yan, H.; Wang, S.-Q.; Lu, H.-Q. [et al.]. 2014. Development of a remotely sensing seasonal vegetation-based Palmer Drought Severity Index and its application of global drought monitoring over 1982–2011. Journal of Geophysical Research: Atmospheres. 119: 9419–9440.

Zargar, A.; Sadiq, R.; Naser, B.; Khan, F.I. 2011. A review of drought indices. Environmental Reviews. 19: 333–349.